10-4-2017

Targeting cysteine thiols for in vitro site-specific glycosylation of recombinant proteins

Yoo Jung Choi
Schulich School of Medicine & Dentistry

Jinhui Zhu
Schulich School of Medicine & Dentistry

Steve Chung
Schulich School of Medicine & Dentistry

Naveed Siddiqui
Schulich School of Medicine & Dentistry

Qingping Feng
Schulich School of Medicine & Dentistry, qfeng@uwo.ca

See next page for additional authors

Video Article

Targeting Cysteine Thiols for *in Vitro* Site-specific Glycosylation of Recombinant Proteins

Yoo Jung Choi*[1], Jinhui Zhu*[1], Steve Chung*[1], Naveed Siddiqui*[1], Qingping Feng[1], Peter B. Stathopulos[1]

[1]Department of Physiology and Pharmacology, Schulich School of Medicine and Dentistry, University of Western Ontario

*These authors contributed equally

Correspondence to: Peter B. Stathopulos at Peter.Stathopulos@schulich.uwo.ca

URL: https://www.jove.com/video/56302
DOI: doi:10.3791/56302

Keywords: Immunology, Issue 128, glycosylation, methanethiosulfonate, cysteine thiol modification, stromal interaction molecule-1, EFSAM, solution nuclear magnetic resonance spectroscopy, mass spectrometry

Date Published: 10/4/2017

Citation: Choi, Y.J., Zhu, J., Chung, S., Siddiqui, N., Feng, Q., Stathopulos, P.B. Targeting Cysteine Thiols for *in Vitro* Site-specific Glycosylation of Recombinant Proteins. *J. Vis. Exp.* (128), e56302, doi:10.3791/56302 (2017).

Abstract

Stromal interaction molecule-1 (STIM1) is a type-I transmembrane protein located on the endoplasmic reticulum (ER) and plasma membranes (PM). ER-resident STIM1 regulates the activity of PM Orai1 channels in a process known as store operated calcium (Ca^{2+}) entry which is the principal Ca^{2+} signaling process that drives the immune response. STIM1 undergoes post-translational *N*-glycosylation at two luminal Asn sites within the Ca^{2+} sensing domain of the molecule. However, the biochemical, biophysical, and structure biological effects of *N*-glycosylated STIM1 were poorly understood until recently due to an inability to readily obtain high levels of homogeneous *N*-glycosylated protein. Here, we describe the implementation of an *in vitro* chemical approach which attaches glucose moieties to specific protein sites applicable to understanding the underlying effects of *N*-glycosylation on protein structure and mechanism. Using solution nuclear magnetic resonance spectroscopy we assess both efficiency of the modification as well as the structural consequences of the glucose attachment with a single sample. This approach can readily be adapted to study the myriad glycosylated proteins found in nature.

Video Link

The video component of this article can be found at https://www.jove.com/video/56302/

Introduction

Store operated calcium (Ca^{2+}) entry (SOCE) is the major pathway by which immune cells take up Ca^{2+} from the extracellular space into the cytosol. In T lymphocytes, T cell receptors located on the plasma membrane (PM) bind antigens which activate protein tyrosine kinases (reviewed in [1,2,3]). A phosphorylation cascade leads to the activation of phospholipase-γ (PLCγ) which subsequently mediates the hydrolysis of membrane phosphatidylinositol 4,5-bisphosphate (PIP_2) into diacylglycerol and inositol 1,4,5-trisphosphate (IP_3). IP_3 is a small diffusible messenger which binds to IP_3 receptors (IP_3R) on the endoplasmic reticulum (ER) thereby opening this receptor channel and permitting Ca^{2+} to flow down the concentration gradient from the ER lumen to the cytosol (reviewed in [4]). Receptor signaling from G protein coupled and tyrosine kinase receptors in a variety of other excitable and non-excitable cell types lead to the same production of IP_3 and activation of IP_3Rs.

Due to the finite Ca^{2+} storage capacity of the ER, the IP_3-mediated release and resultant increase in cytosolic Ca^{2+} is only transient; however, this depletion of the ER luminal Ca^{2+} profoundly effects stromal interaction molecule-1 (STIM1), a type-I transmembrane (TM) protein mostly found on the ER membrane [5,6,7]. STIM1 contains a lumen-oriented Ca^{2+} sensing domain made up of an EF-hand pair and sterile α-motif (EFSAM). Three cytosolic-oriented coiled-coil domains are separated from EFSAM by the single TM domain (reviewed in [8]). Upon ER luminal Ca^{2+} depletion, EFSAM undergoes a destabilization-coupled oligomerization [7,9] which causes structural rearrangements of the TM and coiled-coil domains [10]. These structural changes culminate in a trapping of STIM1 at ER-PM junctions [11,12,13,14] through interactions with PM phosphoinositides [15,16] and Orai1 subunits [17,18]. Orai1 proteins are the PM subunits which assemble to form Ca^{2+} channels [19,20,21,22]. The STIM1-Orai1 interactions at ER-PM junctions facilitate an open Ca^{2+} release activated Ca^{2+} (CRAC) channel conformation which enables the movement of Ca^{2+} into the cytosol from the high concentrations of the extracellular space. In immune cells, the sustained cytosolic Ca^{2+} elevations via CRAC channels induce the Ca^{2+}-calmodulin/calcineurin dependent dephosphorylation of the nuclear factor of activated T-cells which subsequently enters the nucleus and begins transcriptional regulation of genes promoting T-cell activation [1,3]. The process of CRAC channel activation by STIM1 [23,24] via agonist-induced ER luminal Ca^{2+} depletion and the resulting sustained cytosolic Ca^{2+} elevation is collectively termed SOCE [25]. The vital role of SOCE in T-cells is evident by studies demonstrating that heritable mutations in both STIM1 and Orai1 can cause severe combined immunodeficiency syndromes [3,19,26,27]. EFSAM initiates SOCE after sensing ER-luminal Ca^{2+} depletion via the loss of Ca^{2+} coordination at the canonical EF-hand, ultimately leading to the destabilization-coupled self-association [7,28,29].

Glycosylation is the covalent attachment and processing of oligosaccharide structures, also known as glycans, through various biosynthetic steps in the ER and Golgi (reviewed in [30,32,33]). There are two predominant types of glycosylation in eukaryotes: *N*-linked and *O*-linked, depending on the specific amino acid and atom bridging the linkage. In *N*-glycosylation, glycans are attached to the side chain amide of Asn, and in most cases, the initiation step occurs in the ER as the polypeptide chain moves into the lumen [34]. The first step of *N*-glycosylation

is the transfer of a fourteen-sugar core structure made up of glucose (Glc), mannose (Man), and *N*-acetylglucosamine (GlcNAc) (i.e. $Glc_3Man_9GlcNAc_2$) from an ER membrane lipid by an oligosaccharyltransferase [35,36]. Further steps, such as cleavage or transfer of glucose residues, are catalyzed in the ER by specific glycosidases and glycosyltransferases. Some proteins that leave the ER and move into the Golgi can be further processed [37]. *O*-glycosylation refers to the addition of glycans, usually to the side chain hydroxyl group of Ser or Thr residues, and this modification occurs entirely in the Golgi complex [33,34]. There are several *O*-glycan structures which can be made up of *N*-acetylglucosamine, fucose, galactose, and sialic acid with each monosaccharide added sequentially [33].

While no specific sequence has been identified as prerequisite for many types of *O*-glycosylation, a common consensus sequence has been associated with the *N*-linked modification: Asn-X-Ser/Thr/Cys, where X can be any amino acid except Pro [33]. STIM1 EFSAM contains two of these consensus *N*-glycosylation sites: Asn131-Trp132-Thr133 and Asn171-Thr172-Thr173. Indeed, previous studies have shown that EFSAM can be *N*-glycosylated in mammalian cells at Asn131 and Asn171 [38,39,40,41]. However, previous studies of the consequences of *N*-glycosylation on SOCE have been incongruent, suggesting suppressed, potentiated or no effect by this post-translational modification on SOCE activation [38,39,40,41]. Thus, research on the underlying biophysical, biochemical, and structural consequences of EFSAM *N*-glycosylation is vital to comprehending the regulatory effects of this modification. Due to the requirement for high levels of homogeneous proteins in these *in vitro* experiments, a site-selective approach to covalently attach glucose moieties to EFSAM was applied. Interestingly, Asn131 and Asn171 glycosylation caused structural changes that converge within the EFSAM core and enhance the biophysical properties which promote STIM1-mediated SOCE [42].

The chemical attachment of glycosyl groups to Cys thiols has been well-established by a seminal work which first demonstrated the utility of this enzyme-free approach to understanding the site-specific effects of glycosylation on protein function [43,44]. More recently and with respect to STIM1, the Asn131 and Asn171 residues were mutated to Cys and glucose-5-(methanethiosulfonate) [glucose-5-(MTS)] was used to covalently link glucose to the free thiols [42]. Here, we describe this approach which not only uses mutagenesis to incorporate site specific Cys residues for modification, but also applies solution nuclear magnetic resonance (NMR) spectroscopy to rapidly assess both modification efficiency and structural perturbations as a result of the glycosylation. Notably, this general methodology is easily adaptable to study the effects of either *O*- or *N*-glycosylation of any recombinantly produced protein.

Protocol

1. Polymerase chain reaction (PCR)-mediated site-directed mutagenesis for the incorporation of Cys into a bacterial pET-28a expression vector.

1. Determine the concentration of the pET-28a vector (i.e. double stranded DNA) using a ultraviolet (UV) extinction coefficient of 0.020 (µg/mL) cm^{-1} at 260 nm.
2. Synthesize a pair of complementary mutagenic primers for each Cys mutation such that *i*) there are a minimum of 15 nucleotides complementary to the template prior to the first base mismatch and 15 nucleotides complementary to the template after the final base mismatch, *ii*) total primer length does not exceed 45 nucleotides, and *iii*) a guanine or cytosine is located at the first and last nucleotide position of each primer (Table 1). Ensure primer synthesis is performed using a 0.025 µmol scale and cartridge purification.
3. Using a high fidelity DNA polymerase, set up two 20 µL PCR reaction mixtures: one containing the forward primer and the second containing the reverse primer. Prepare each mixture to contain final concentrations of 1x PCR buffer with 1.5 mM $MgCl_2$, 0.2 mM dNTPs, 0.5 µM primer, 0.4 µL DMSO, 1.25 ng/µL template DNA, 0.02 U/µL high fidelity DNA polymerase.
4. Thermally cycle the separate mixtures using a three-step protocol: 98 °C for 30 s (denaturing), 53 - 56 °C for 30 s (annealing), 72 °C for 30 s $kilobase(kb)^{-1}$ (extension) of the template DNA. Repeat the temperature program for 5 cycles and add a final 72 °C extension step for 7.5 min.
5. After the initial PCR with forward and reverse primers in separate tubes, combine the products into a single tube (i.e. 40 µL total) and continue the PCR reaction for an additional 20 cycles using the same cycling parameters as described in step 1.4.
6. Electrophorese 15 µL of the PCR reaction mixture on a 1% (w/v) agarose gel using 0.5x Tris, acetic acid, ethylene diamine tetra acetic acid (EDTA) running buffer (TAE). As controls, electrophorese an equivalent amount of template DNA which has not been amplified by PCR and an aliquot of reference DNA ladder which contains marker bands both greater and less than the expected PCR product size.
7. After electrophoresis at 120 V for 40 min, submerge the gel in water containing 0.5 µg/mL ethidium bromide and shake for 30 min at room temperature. Confirm the full-length template has been amplified by the mutagenic primers as an increase in the relative ethidium bromide fluorescent intensity of the amplified band compared to the control template band under UV light (302 nm).
    1. If no amplification is apparent, repeat the PCR after adjusting annealing temperature in 0.5 °C increments between the 53 - 56 °C temperature range.
8. Upon confirmation of amplification of the template by the mutagenic primers, treat the remaining ~25 µL of the PCR reaction mixture with the DpnI restriction enzyme to digest the methylated template DNA. Use DpnI at 0.5 µL (10 units) per 25 µL PCR reaction mixture and a final concentration of 1× DpnI reaction buffer. Incubate for 2.5 h at 37 °C.
9. Following template digestion, add ~5 - 10 µL of the digested mixture to 100 µL of heat shock competent DH5α *Esherichia coli* cells in a 1.75 mL microcentrifuge tube. Incubate the cell-DNA mixture on ice for 60 min.
10. Heat shock the cell-DNA mixture in the microcentrifuge tube at 42 °C for 45 s on a dry heat block. After incubating the mixture on ice for 3 min, add 900 µL of room temperature Luria-Bertani broth (LB) to the cells and transfer the total cell suspension into a sterile 14 mL round-bottom tube.
11. Incubate the cell suspension at 37 °C for 90 min with constant shaking at 190 rpm.
12. Subsequently, transfer the cell suspension back into a 1.75 mL microcentrifuge tube and centrifuge at 10,000 x g for 5 min at room temperature.
13. After the centrifugation, remove 900 µL of the supernatant and resuspend the bacterial cells by gentle pipetting in the remaining 100 µL of LB.
14. Transfer the resultant concentrated cell suspension onto an LB-agar plate containing antibiotic which is selective for the expression vector (i.e. 60 µg/mLKanamycin). Aseptically spread the suspension evenly on the agar plate and incubate for ~16 h at 37 °C.

15. The following day, inoculate a single colony from the plate into 5 mL of liquid LB containing the antiobiotic selection pressure (i.e. 60 µg/mL Kanamycin). Grow the liquid culture overnight at 37 °C with constant shaking at 37 °C.
16. Isolate and purify the propagated plasmid from the *E. coli* cells using a commercially available kit based on the alkaline lysis procedure [45].
17. Confirm the mutation of interest is present and in the proper reading frame by Sanger DNA sequencing of the plasmid [46].

2. Uniform ^{15}N-labeled protein expression in BL21 ΔE3 *Escherichia coli* .

NOTE: Different recombinant proteins require different expression conditions. The following is the optimized procedure for expression of the human STIM1 EFSAM protein.

1. Transform the expression vector harboring the Cys mutations (i.e. pET-28a-EFSAM) into BL21 ΔE3 codon (+) heat shock competent cells and plate on LB-agar plates containing the antibiotic selection pressure as described in steps 1.9-1.14) with the following modifications: directly plate a 150 µL aliquot out of the ~1,000 µL total cell suspension on the LB-agar plate without the need for concentrating the cells in a microcentrifuge tube by centrifugation.
2. The following day, aseptically transfer a single colony into a 200 mL Erlenmeyer flask containing 20 mL of LB supplemented with the appropriate antibiotic (i.e. 60 µg/mL kanamycin for pET-28a-EFSAM). Grow this liquid starter culture overnight (i.e. ~16 h) at 37 °C with constant shaking at ~ 190 rpm.
3. On the same day as step 2.2, prepare M9 medium for ^{15}N-labeled protein expression by autoclaving 1 L of M9 buffer salts (i.e. 42 mM Na_2HPO_4, 22 mM KH_2PO_4, 8.6 mM NaCl, pH 7.4) in a 4 L Erlenmeyer flask. Once cool, filter a mixture of 20% (w/v) D-glucose, 1 M $CaCl_2$, 1 M thiamine, 1 M $MgSO_4$, 1 mg/mL biotin and 0.2 g/mL ^{15}N-NH_4Cl through a 0.2 µm sterile syringe filter into the 1 L sterile M9 salt solution so that the final concentrations of these components are 0.2% (w/v) D-glucose, 100 µM $CaCl_2$, 50 µM thiamine, 1 mM $MgSO_4$, 1 µg/mL biotin and 1 mg/mL ^{15}N-NH_4Cl.
4. The next day, aseptically transfer the 20 mL overnight liquid starter culture into a 50 mL sterile conical tube and centrifuge at 2,400 ×*g* for 15 min to pellet the cells.
5. After decanting the LB medium, resuspend the resulting cell pellet in 10 mL of M9 minimal medium and transfer the resuspended pellet mixture into 1 L of M9 minimal medium with antibiotic (i.e. 60 µg/mL kanamycin).
6. Grow the 1 L of M9 minimal medium containing the bacterial starter culture at 37 °C and ~190 rpm constant shaking until the optical density at 600 nm (OD600) reaches ~0.6-0.8.
7. When the specfified OD600 range is reached, add 200 µM of isopropyl β-D-1-thiogalactopyranoside (IPTG) to induce protein expression.
8. After IPTG addition, continue incubating the cells for protein expression at ambient temperature with constant shaking at ~190 rpm for ~16 h (i.e. overnight).
9. The next day, harvest the bacteria by centrifugation at ~10,000 ×g, 4 °C for 30 min.
10. Decant the LB and transfer the cell pellet into a 50 mL conical tube. Store the pellet at -80 °C until purification.

3. Purification of recombinant protein from *E. coli*.

NOTE: Different recombinant proteins require distinct purification procedures. The following is the protocol for 6×His-tagged EFSAM purification from inclusion bodies expressed from the pET-28a construct.

1. Manually homogenize the frozen bacterial cell pellet in 6 M guanidine-HCl, 20 mM Tris-HCl (pH 8) and 5 mM β-mercaptoethanol using a motorized 10 mL transfer pipette. Add approximately 40 mL of guanidine-HCl per 5 mL of wet cell pellet for this step.
2. Following a 90 min incubation at ambient temperature with constant rotation in a hybridization oven, centrifuge the mixture at ~15,000 ×g, 8 °C for 40 min to separate the insoluble cell debris (*i.e.* pellet) from the soluble protein mixture (i.e. supernatant).
3. Add 750 µL of a 50% (v/v) Ni^{2+}-nitrilotriacetic acid agarose bead slurry to the clarified lysate and incubate for another 90 min at room temperature with inversion in a hybridization oven.
4. Subsequently, capture the 6×His-tagged protein bound to the Ni^{2+} by collecting the agarose beads in a gravity flow protein purification column. Allow the lysate to flow through the column completely prior to moving to step 3.5.
5. Wash the collected beads three times with 10 mL of 6 M urea, 20 mM Tris-HCl pH 8 and 5 mM β-mercaptoethanol. Ensure that the entire 10 mL passes through the column prior to each subsequent 10 mL wash.
6. Elute the proteins in a series of 2 mL fractions using 6 M urea, 20 mM Tris-HCl pH 8, 300 mM imidazole, and 5 mM β-mercaptoethanol with a 90 s incubation time between fractions. Ensure that the entire 2 mL passes through the column prior to each subsequent elution step.
7. At this stage, confirm the protein of interest is present in the eluted fractions by Coomassie blue-stained sodium dodecyl sulfate polyacrylamide gel electrophoresis (SDS-PAGE) using the method of Laemmli [47]. Assess the protein size, quantity and purity by comparison against standard molecular weight marker bands which are both less than and greater than the expected molecular weight of the protein of interest.
8. Pool the eluted protein fractions into a dialysis membrane with a 3,500 Da molecular weight cutoff and incubate in 1 L refolding buffer (20 mM Tris, 300 mM NaCl, 1 mM DTT, 5 mM $CaCl_2$, pH 8) at 4 °C overnight while the buffer is being stirred by a magnetic stirrer.
9. After ~16 h of refolding time, add ~1 U of thrombin per mg of protein directly to the dialysis bag and incubate at 4 °C for an additional ~24 h.
10. Verify the extent of the 6×His tag cleavage by Coomassie-blue staining of ~15 µL protein aliquots taken from the dialysis bag before and after incubation with thrombin which are electrophoresed on denaturing polyacrylamide gels (SDS-PAGE) using the method of Laemmli [47]. If a ~2 kDa shift in the migration is observed corresponding to the molecular weight of the cleaved 6×His tag, continue to step 3.11; if a fraction of undigested protein remains that is detectable by Coomassie-blue staining, add ~0.2 U of thrombin per mg of protein directly to the dialysis bag and incubate at 4 °C for an additional ~24 h.
11. Use size exclusion or ion exchange chromatography to further purify the protein. For anion exchange chromatography of EFSAM, remove the protein solution from the dialysis bag and concentrate ~10-fold using an ultrafiltration centrifugal concentrator with a 10,000 Da molecular weight cutoff. Subsequently, re-dilute the solution ~20-fold in a NaCl-free buffer (20 mM Tris, 5 mM $CaCl_2$, 1 mM DTT, pH 8).
12. Equilibrate a prepacked anion exchange column with 10 column volumes of the NaCl-free buffer described in step 3.11. Equilibrate using buffer loaded into a luer-lock syringe containing no air bubbles by pushing the solution through the column in a dropwise manner and

avoiding syringe pressures which cause steady streams of solution exiting the column. Use a strong anion exchanger (e.g. crosslinked agarose with quaternary ammonium functional groups).
13. Load the protein solution diluted into NaCl-free buffer (step 3.11) onto the column as described in step 3.12.
14. Elute the proteins in a gradient [i.e. 0 - 60% (v/v)] of increasing NaCl buffer (20 mM Tris, 1 M NaCl, 5 mM $CaCl_2$, 1 mM DTT, pH 8) using a two-pump fast protein liquid chromatography (FPLC) system. Set the FPLC system to collect ~1-1.5 mL fractions and monitor the protein elution profile using UV 280 nm absorbance and a flow rate 0.5 mL/min.
15. Identify the elution peaks and fractions containing the protein of interest as well as protein purity by Coomassie blue-stained SDS-PAGE gels using the method of Laemmli [47].
16. Pool fractions showing > 95% (i.e. taken as fractions which show only a single protein band on Coomassie-blue stained gels) into a dialysis bag and exchange into experimental buffer of interest by dialysis as described in step 3.8.

4. Chemical attachment of glucose-5-MTS to protein by dialysis.

1. Prepare a 55 mM stock solution of N-(β-D-glucopyranosyl)-N'-[2-methanethiosulfonyl)ethyl]urea (glucose-5-MTS) by dissolving 10 mg of the compound in 500 µl of 100% (v/v) DMSO. Store unused glucose-5-MTS solubilized in DMSO at -20 °C.
2. Prepare the protein sample for modification by dialyzing 1.5 mL of ~60 µM protein into 1 L of modification buffer made up of 20 mM MOPS, 150 mM NaCl, 5 mM $CaCl_2$ and 0.1 mM TCEP, pH 8.3. Use a dialysis membrane molecular weight cutoff which is smaller than the size of protein being modified (e.g. use a 3,500 Da cutoff for the ~17,500 Da EFSAM).
3. After 24 h at 4 °C, transfer the sample from the dialysis bag into a microcentrifuge tube. Add the DMSO-solubilized glucose-5-MTS to a final concentration of 2 mM.
4. Incubate the sample in the dark for 1 h at ambient temperature. During the 1 h incubation period, mix the solution by gentle tapping of the tube every 10 min.
5. Subsequently, re-exchange the protein into the final experimental buffer containing no reducing agent by dialysis at 4 °C as described in step 4.2 or by centrifugal ultrafiltration. For the ultrafiltration procedure, concentrate the ~1.5 mL protein sample to < 0.5 mL and subsequently dilute in the same concentrator with the experimental buffer. Repeat this concentration-dilution step two additional times so that the total exchange is a minimum of 30×30×30 = 27,000-fold. For EFSAM, use 20 mM Tris, 150 mM NaCl, 5 mM $CaCl_2$, pH 7.5 as the experimental buffer.
6. Prepare the sample for electrospray ionization mass spectrometry by dialysis or ultrafiltration exchange as described in steps 4.2 and 4.5, respectively, into 25 mM ammonium bicarbonate or 25 mM ammonium acetate. If using dialysis, ensure you exchange at least three times to remove any residual NaCl and $CaCl_2$ salts.
7. Determine the accurate mass (i.e. ± 1 Da) of the protein of interest using electrospray ionization mass spectrometry [48,49]. Expect each covalent glucose addition to a Cys thiol via the methanethiosulfonate chemical to add 281.3 Da to the protein mass (i.e. add 360.4 Da for the glucose-5-MTS and subtract 79.1 Da for the CH_3SO_2 leaving group during covalent attachment).

5. Solution NMR assessment of modification efficiency and structural perturbations.

1. Ensure the concentration of the modified protein is > 100 µM after the glucose attachment and final buffer exchange. For EFSAM, estimate protein concentration using a UV extinction coefficient at 280 nm of 1.54 (mg mL^{-1}) cm^{-1}.
2. Supplement the protein solution with 60 µM of 4,4-dimethyl-4-silapentane-1-sulfonic acid (DSS) for shimming and pulse calibration and 10% (v/v) D_2O for the signal lock. For high signal-to-noise use 600 µL samples in frequency-matched 5 mm NMR tubes, inserted into a minimum 600 MHz spectrometer equipped with a triple resonance HCN cryogenic probe.
3. Collect standard ^{1}H-^{15}N HSQC spectra as previously detailed [50,51] at temperature, ^{1}H and ^{15}N sweep widths, transient and increment settings suitable for the particular sample. For EFSAM spectra, use 20 °C, 256 ^{1}H transients, 64 ^{15}N dimension increments and ^{1}H and ^{15}N sweep widths set to 8,000 and 1,800 Hz, respectively.
4. Following the acquisition of the glycosylated protein spectrum, add dithiothreitol (DTT) to the NMR sample from a 1 M stock to a final concentration of 15 mM. The DTT removes the glucose moiety from the protein by reduction of the disulfide-mediated attachment.
5. Acquire a second ^{1}H-^{15}N HSQC under these reduced/unmodified conditions, providing a reference spectrum to assess modification efficiency and structural perturbations caused by the glucose attachment.
6. Process the NMR data using NMRPipe as detailed previously [52]. Ensure that processing minimally includes data conversion, phasing, solvent suppression, Fourier transform and initial visualization of the spectra.
7. Assess modification efficiency by measuring the amide peak intensities and chemical shift values in the modified and reduced spectra using the NEASY plugin on CARA [53]. Ensure to evaluate the peak intensity of the Cys amide both in the glucose attached and reduced spectra. If the Cys amide cannot be reliably located in both spectra, use the intensities of residues adjacent to the Cys as a readout.
8. Calculate the efficiency as the intensity of the amide from the Cys-modified spectrum divided by the intensity of the amide from the Cys-reduced (i.e. DTT-treated) spectrum, multiplied by 100:
   $Efficiency = \frac{I_M}{I_R} \times 100$, where I_M is the intensity of the amide in the Cys-modified spectrum and I_R is the intensity of the amide in the Cys-reduced spectrum. Alternatively, evaluate the mean efficiency over several amide peaks:
   $Mean\ Efficiency = \frac{1}{n}\sum_{i=1}^{n} Efficiency_i$, where $Efficiency_i$ is the separately determined efficiency calculated for each residue, *i,* and *n* is the total number of residues used in the calculation.
9. Calculate chemical shift perturbations (CSP) from the chemical shift differences between the two spectra observed in the ^{15}N and ^{1}H dimensions of each peak and normalizing for the larger ^{15}N chemical shift range using the following equation:
   $CSP = \sqrt{\Delta H^2 + (0.14 \times \Delta N)^2}$, where ΔH is the ppm change in the proton dimension and ΔN is the ppm change in the nitrogen dimension.

Representative Results

The first step of this approach requires the mutagenesis of the candidate glycosylation residues to Cys residues which can be modifiable using the glucose-5-MTS. EFSAM has no endogenous Cys residues, so no special considerations need to be made prior to the mutagenesis. However, native Cys residues must be mutated to non-modifiable residues prior to performing the described chemistry. To minimally effect the native structure, we suggest performing a global sequence alignment of the protein of interest and determining which other residues are found most frequently at the endogenous Cys position(s). Cys mutation to these other residues which occur naturally in other organisms may have the least impact on protein structure. If the endogenous Cys residue is strictly conserved, we suggest mutating to Ser which is the most structurally similar to Cys. **Figure 1** shows a typical PCR mutagenesis gel evaluating the success of the PCR reaction, with the amplified DNA sample demonstrating several-fold higher intensity than a control amount of unamplified template pET-28a DNA which was used for PCR. The next steps include template DNA digestion and transformation into *E. coli* for plasmid repair. After plasmid propagation in liquid culture, plasmid isolation and confirmation of the mutation(s) by sequencing, the mutated vector may be used for protein expression. **Figure 2A** shows a typical elution profile of EFSAM from the anion exchange column relative to increasing NaCl concentrations. **Figure 2B** shows the purity of EFSAM on Coomassie blue-stained SDS-PAGE gels.

After acquiring pure protein, a series of dialysis steps is used to attach the glucose moiety via the MTS reaction with the free thiol. **Figure 3A** shows an image of the typical setup of a small protein volume sealed in the dialysis membrane by membrane clips and contained in a large 1 L beaker containing the buffer of interest. An initial check of the success of the modification may be performed by mass spectrometry. **Figure 3B** shows a representative electrospray mass spectrum of EFSAM modified at a single Cys thiol. Following establishment of the protocol for a specific protein, modification efficiency and structural perturbations can be assessed from a single uniformly ^{15}N-labeled sample. The ^{1}H-^{15}N-HSQC spectrum is acquired before and after the addition of the reducing agent DTT (**Figure 4A**). Calculations of the modification efficiency can be made via a comparison of the amide peak intensities in the modified and reduced spectra as detailed in protocol step 5.8 (**Figure 4B**). Finally, when chemical shift assignments are known for a protein, the CSPs which correlate with the structural changes can be calculated as detailed in step 5.9 (**Figure 4C**).

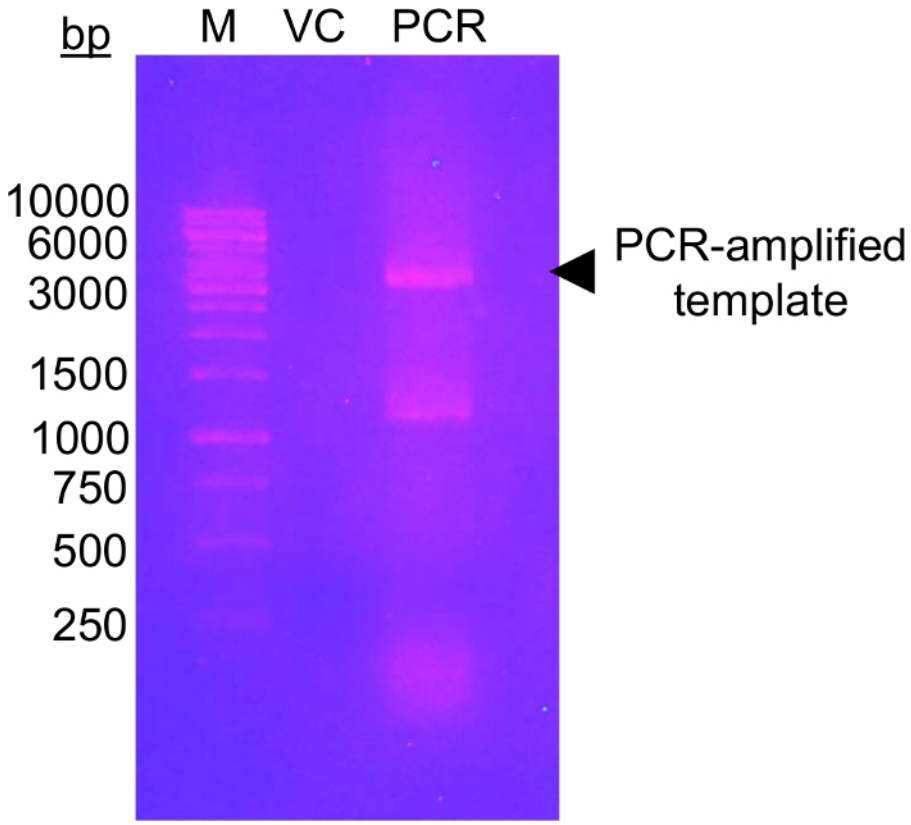

Figure 1: DNA agarose gel showing amplification check of template vector with mutagenic primers.
The image shows a 1.0% (w/v) agarose gel with DNA marker (M), vector control (VC) and PCR-amplified template (PCR). The DNA was separated by electrophoresis at 120 V for 45 min in 0.5x TAE buffer. A total of 0.5 ng of VC was loaded, equivalent to the amount of template loaded into the PCR lane. The gel was stained using ethidium bromide (~0.5 µg/mL) for 20 min prior to visualization under UV light (302 nm). The gel shows a high level of amplified DNA close to the expected size of the vector (black arrowhead). The second band in the PCR lane running between the 1,000 and 1,500 bp marker bands likely represents a non-specifically amplified PCR product. The intensity level of amplified DNA must be higher than the VC intensity level to be deemed successful. Several other DNA dyes can be used as less mutagenic, safer alternatives to ethidium bromide staining (see for example [57]). Please click here to view a larger version of this figure.

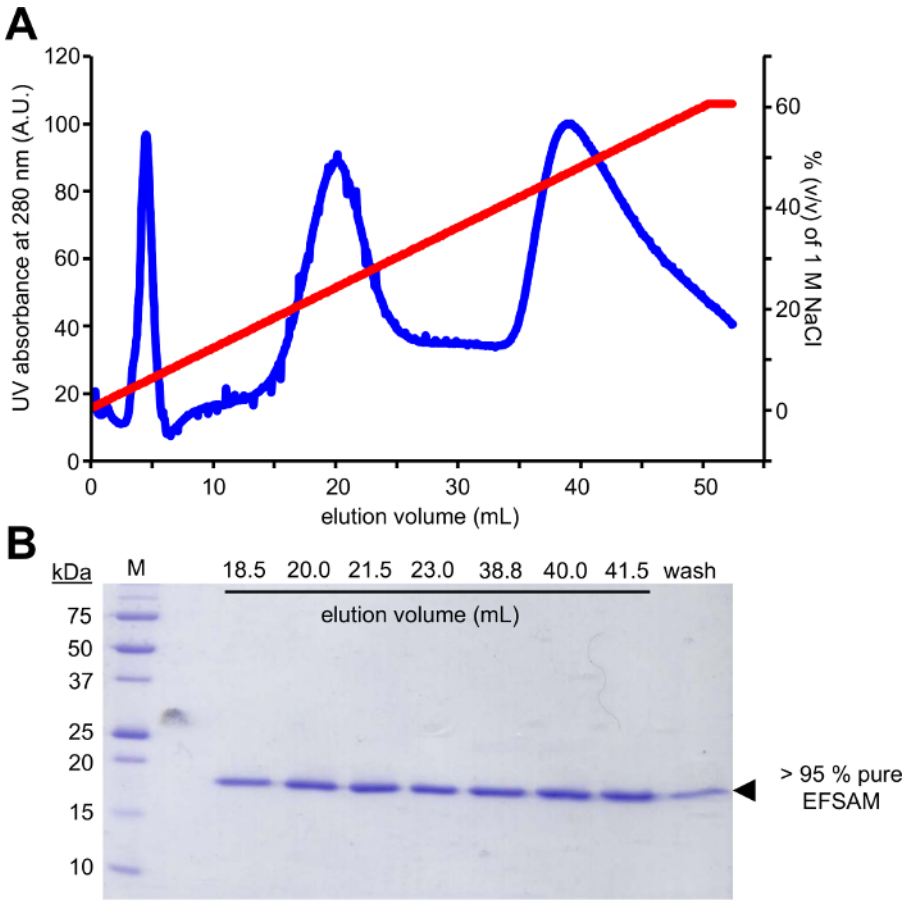

Figure 2: Typical chromatographic purification and purity check for STIM1 EF-SAM.
(A) Anion exchange chromatography elution profile of STIM1 EF-SAM. After manual binding EF-SAM to the anion exchange column (Q FF) at basic pH and low NaCl concentration with a syringe, and AKTA FPLC (GE Healthcare) is used to elute the protein with a NaCl gradient. The elution is monitored by the AKTA using the UV 280 nm signal over a 0-60% (v/v) gradient of 1 M NaCl. ***(B)*** Coomassie blue-stained SDS-PAGE gel of elution fractions from (A). The denaturing protein gel reveals that EF-SAM elutes in two major peaks at ~250 mM and ~450 mM NaCl. The purification protocol yields > 95% pure EF-SAM as evidenced by the lack of any contaminant band showing up in the Coomassie blue-stained gel. Please click here to view a larger version of this figure.

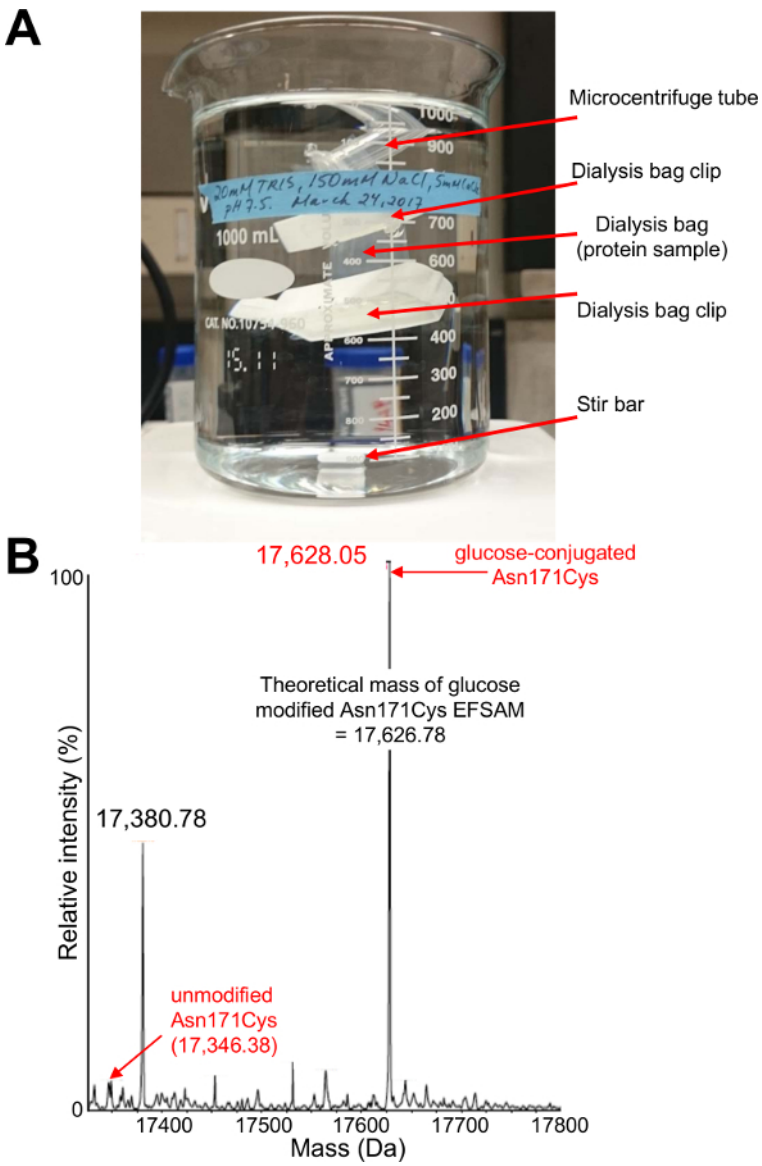

Figure 3: Dialysis setup and confirmation of *in vitro* protein glycosylation.
(A) Typical dialysis setup used for *in vitro* attachment of glucose to the Cys thiol via the MTS reactivity. The image shows ~1.5 mL of protein contained within dialysis tubing buffered against ~ 1 L of experimental buffer. It is important that the buffer is constantly stirred to ensure complete exchange. The image shows a microcentrifuge tube clipped to the excess dialysis tubing to prevent sinking of the dialysis bag and damage by the rotating stir bar. ***(B)*** Electrospray ionization mass spectrum of the modified Asn171Cys EF-SAM protein. Mass spectrometry is a convenient and accurate approach to assess whether the modification procedure was successful. A typical mass chromatogram is shown with the theoretical and measured masses of unmodified and modified Asn171Cys EF-SAM indicated. The majority of the sample mass corresponds to a macromolecule which is within ~1.3 Da of the expected theoretical mass of glucose-conjugated Asn171Cys EF-SAM. The data in (*B*) is replotted and modified from [42]. Please click here to view a larger version of this figure.

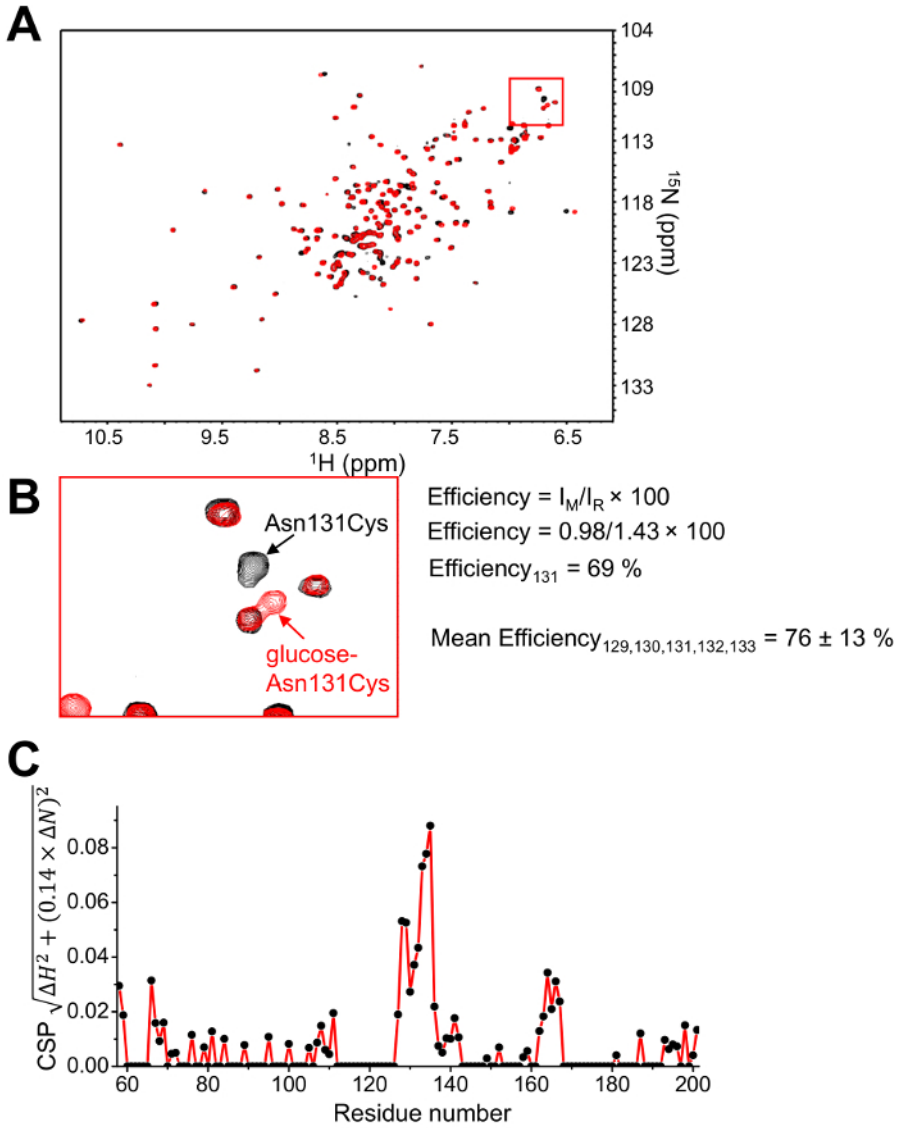

Figure 4: Solution NMR assessment of modification efficiency and structural perturbations from a single NMR sample. ***(A)*** ^{1}H-^{15}N-HSQC spectral overlay of glucose-conjugated Asn131Cys EFSAM before (red crosspeaks) and after (black crosspeaks) the addition of 15 mM DTT. The overlay clearly shows several residue-specific amide chemical shift changes indicative of both modification of the protein and structural perturbations. The red box shows the location of the Asn131Cys amide. ***(B)*** Zoomed view of the ^{1}H-^{15}N-HSQC region containing the Asn131Cys amide. The intensity of the Asn131Cys amide peak in the modified spectrum (I_M) is divided by the intensity in the reduced (unmodified) spectrum (I_R) for the calculation of efficiency (shown). A calculation of the mean efficiency of several effected residues provides a better estimate of efficiency, including an error estimate. The mean efficiency is shown for Asn131Cys EFSAM based on 5 residues (i.e. 129-133). ***(C)*** Normalized chemical shift perturbations caused by glucose conjugation to the Asn131Cys EFSAM protein. The set of HSQC experiments collected on a single sample before and after supplementing with reducing agent not only provides a convenient estimate of modification efficiency by peak intensity analysis [shown in *(B)*], but also provides data for evaluation of the structural changes associated with the modification. Glucose conjugation causes the largest perturbations localized near position 131; however, this analysis reveals perturbations which are unexpected solely based on sequence proximity, indicating the value in this analysis. The data in (*C*) are replotted and modified from [42]. Please click here to view a larger version of this figure.

STIM1 mutation[a]	direction[b]	DNA sequence[c]
Asn131Cys	forward	5'-GTCATCAGAAGTATACTGTTGGACCGTGGATGAGG-3'
Asn131Cys	reverse	5'-CCTCATCCACGGTCCAACAGTATACTTCTGATGAC-3'
Asn171Cys	forward	5'-CCAAGGCTGGCTGTCACCTGCACCACCATGACAGGG-3'
Asn171Cys	reverse	5'-CCCTGTCATGGTGGTGCAGGTGACAGCCAGCCTTGG-3'
[a]STIM1 amino acid numbering based on NCBI accession AFZ76986.1.		
[b]The 'reverse' primer corresponds to the reverse complement sequence of the 'forward' primer.		
[c]The underlined codon triplet corresponds to the Cys mutation.		

Table 1. Example oligonucleotide (primer) sequences for Asn to Cys mutagenesis within the pET-28a STIM1 EFSAM construct.

Discussion

Protein glycosylation is a post-translational modification where sugars are covalently attached to polypeptides primarily through linkages to amino acid side chains. As many as 50% of mammalian proteins are glycosylated [54], where the glycosylated proteins can subsequently have a diverse range of effects from altering biomolecular binding affinity, influencing protein folding, altering channel activity, targeting molecules for degradation and cellular trafficking, to name a few (reviewed in[33]). The important role of glycosylation in mammalian physiology is evident by the several hundreds of proteins evolved to build the full diversity of mammalian glycan structures [33]. Altered *N*- and *O*-glycosylation patterns have been associated with numerous disease states including prostate (increased and decreased), breast (increased and decreased), liver (increased), ovarian (increased), pancreatic (increased) and gastric cancers (increased) [55]. Furthermore, glycosylation of Tau, huntingtin, α-synuclein has been found to regulate toxicity of these proteins associated with Alzheimer's, Huntington's and Parkinson's diseases [56], and a group of congenital disorders of glycosylation have been identified resulting from heritable defects in enzymes which mediate glycosylation [54]. Thus, understanding the precise biophysical, biochemical and structural effects of glycosylation has the potential to tremendously impact our understanding of protein regulation and function in health and disease.

The ten sugar building blocks which lead to the diversity of glycan structures found in the mammalian glycome include fucose, galactose, glucose, *N*-acetylgalactosamine, *N*-acetylglucosamine, glucuronic acid, iduronic acid, mannose, sialic acid and xylose [33]. While *N*-glycosylation invariably links an *N*-acetylglucosamine sugar directly to the protein, *O*-glycosylation can result from any of *N*-acetylgalacotose, *N*-acetylglucosamine, xylose, fucose, glucose or galactose covalently linked to the polypeptide. To begin to understand how these sugars immediately adjacent to the protein surface affect the biophysical and structural properties, we describe herein an approach to site-selectively attach sugars to Cys residues via the thiols engineered into the protein sequence. Here, the residues that are endogenously glycosylated are replaced by Cys and modified *in vitro* via a simple chemical approach. In this manner, single and multiple glycosylation sites may be assessed to tease out the contribution of each specific site as well as the cumulative modifications to the folding and stability as well as the overall structure and function of the protein.

Recently, this approach was successfully used with EFSAM to individually and cumulatively assess the role of the Asn131 and Asn171 *N*-glycosylation sites [42]. Mutation to Cys and covalent attachment of glucose to the Asn131 or Asn171 sites revealed a decreased Ca^{2+} binding affinity and suppressed stability. When the two sites were simultaneously modified with the glucose attachment, the decreases in binding affinity and stability were potentiated leading to enhanced oligomerization propensity *in vitro*. Structurally, the approach described herein showed that the Asn131 or Asn171 modifications mutually perturb the core α8 helix located on the SAM domain, immediately adjacent to the EF-hand pair. This structural analysis expounds how glucose modifications on the surface of the protein lead to a converging and potentiated structural change within the EF-hand:SAM interface which ultimately destabilizes the protein and enhances SOCE [42].

While the application of this site-selective approach helped shed light on how a monosaccharide close to the surface of EFSAM effects folding, stability and structure, this procedure can easily be modified to attach longer carbohydrates specific to ER, Golgi and PM localization (i.e. glycosylation states of different maturity), provided there is a reliable source for these carbohydrates containing functional groups which can link to thiols such as MTS. MTS is preferable since the thiol modification is reversible using a reducing agent and a reference spectrum can be easily acquired. This approach can also be adapted to link other post-translational moieties to the protein such as lipids. At the same time, there are several limitations to this approach which should be considered. First, the method relies on mutation of glycosylation sites to Cys which may affect structure, stability and folding even in the absence of any glucose modification. Similarly, native Cys residues in the protein must also be mutated to prevent glucose attachment at non-glycosylated sites. Additionally, the addition of Cys residues often promotes inclusion body formation in bacteria due to Cys crosslinking and misfolding, making purification more challenging. Nevertheless, this site-selective Cys-crosslinking approach described herein provides a controlled means to tease out the structural, biochemical and biophysical effects of specific glycosylation sites in experiments which require high levels of homogeneous protein. The effects of non-native Cys residues on the structure, stability and folding can be simply ascertained in the absence of any modifications by comparison to wild-type protein attributes [42]. Taken together with functional data obtained in eukaryotic cells which express modification-blocking mutant versions of the protein (e.g. Asn-to-Ala), the presently described approach will yield new insights into the structural mechanisms of protein regulation by post-translational modifications.

Acknowledgements

This research was supported by the Natural Sciences and Engineering Research Council of Canada (05239 to P.B.S.), Canadian Foundation for Innovation/Ontario Research Fund (to P.B.S.), Prostate Cancer Fight Foundation - Telus Ride for Dad (to P.B.S.) and Ontario Graduate Scholarship (to Y.J.C. and N.S.).

References

1. Feske, S. Calcium signalling in lymphocyte activation and disease. *Nat Rev Immunol.* **7** (9), 690-702 (2007).
2. Feske, S., Skolnik, E.Y., & Prakriya, M. Ion channels and transporters in lymphocyte function and immunity. *Nat Rev Immunol.* **12** (7), 532-547 (2012).
3. Shaw, P.J., & Feske, S. Physiological and pathophysiological functions of SOCE in the immune system. *Front Biosci (Elite Ed).* **4**, 2253-2268 (2012).
4. Seo, M.D., Enomoto, M., Ishiyama, N., Stathopulos, P.B., & Ikura, M. Structural insights into endoplasmic reticulum stored calcium regulation by inositol 1,4,5-trisphosphate and ryanodine receptors. *Biochim Biophys Acta.* **1853** (9), 1980-1991 (2015).
5. Stathopulos, P.B., & Ikura, M. Structural aspects of calcium-release activated calcium channel function. *Channels (Austin).* **7** (5), 344-353 (2013).
6. Stathopulos, P.B., & Ikura, M. Structure and function of endoplasmic reticulum STIM calcium sensors. *Curr Top Membr.* **71**, 59-93 (2013).
7. Stathopulos, P.B., Li, G.Y., Plevin, M.J., Ames, J.B., & Ikura, M. Stored Ca2+ depletion-induced oligomerization of stromal interaction molecule 1 (STIM1) via the EF-SAM region: An initiation mechanism for capacitive Ca2+ entry. *J Biol Chem.* **281** (47), 35855-35862 (2006).
8. Stathopulos, P.B., & Ikura, M. Store operated calcium entry: From concept to structural mechanisms. *Cell Calcium.* (2016).
9. Stathopulos, P.B., & Ikura, M. Structurally delineating stromal interaction molecules as the endoplasmic reticulum calcium sensors and regulators of calcium release-activated calcium entry. *Immunol Rev.* **231** (1), 113-131 (2009).
10. Muik, M. *et al.* STIM1 couples to ORAI1 via an intramolecular transition into an extended conformation. *EMBO J.* **30** (9), 1678-1689 (2011).
11. Luik, R.M., Wang, B., Prakriya, M., Wu, M.M., & Lewis, R.S. Oligomerization of STIM1 couples ER calcium depletion to CRAC channel activation. *Nature.* **454** (7203), 538-542 (2008).
12. Luik, R.M., Wu, M.M., Buchanan, J., & Lewis, R.S. The elementary unit of store-operated Ca2+ entry: local activation of CRAC channels by STIM1 at ER-plasma membrane junctions. *J Cell Biol.* **174** (6), 815-825 (2006).
13. Wu, M.M., Buchanan, J., Luik, R.M., & Lewis, R.S. Ca2+ store depletion causes STIM1 to accumulate in ER regions closely associated with the plasma membrane. *J Cell Biol.* **174** (6), 803-813 (2006).
14. Liou, J., Fivaz, M., Inoue, T., & Meyer, T. Live-cell imaging reveals sequential oligomerization and local plasma membrane targeting of stromal interaction molecule 1 after Ca2+ store depletion. *Proc Natl Acad Sci U S A.* **104** (22), 9301-9306 (2007).
15. Calloway, N. *et al.* Stimulated association of STIM1 and Orai1 is regulated by the balance of PtdIns(4,5)P(2) between distinct membrane pools. *J Cell Sci.* **124** (Pt 15), 2602-2610 (2011).
16. Korzeniowski, M.K. *et al.* Dependence of STIM1/Orai1-mediated calcium entry on plasma membrane phosphoinositides. *J Biol Chem.* **284** (31), 21027-21035 (2009).
17. Park, C.Y. *et al.* STIM1 clusters and activates CRAC channels via direct binding of a cytosolic domain to Orai1. *Cell.* **136** (5), 876-890 (2009).
18. Yuan, J.P. *et al.* SOAR and the polybasic STIM1 domains gate and regulate Orai channels. *Nat Cell Biol.* **11** (3), 337-343 (2009).
19. Feske, S. *et al.* A mutation in Orai1 causes immune deficiency by abrogating CRAC channel function. *Nature.* **441** (7090), 179-185 (2006).
20. Prakriya, M. *et al.* Orai1 is an essential pore subunit of the CRAC channel. *Nature.* **443** (7108), 230-233. (2006).
21. Vig, M. *et al.* CRACM1 multimers form the ion-selective pore of the CRAC channel. *Curr Biol.* **16** (20), 2073-2079 (2006).
22. Vig, M. *et al.* CRACM1 is a plasma membrane protein essential for store-operated Ca2+ entry. *Science.* **312** (5777), 1220-1223 (2006).
23. Liou, J. *et al.* STIM is a Ca2+ sensor essential for Ca2+-store-depletion-triggered Ca2+ influx. *Curr Biol.* **15** (13), 1235-1241. (2005).
24. Roos, J. *et al.* STIM1, an essential and conserved component of store-operated Ca2+ channel function. *J Cell Biol.* **169** (3), 435-445. Epub 2005 May 2002. (2005).
25. Putney, J.W., Jr. A model for receptor-regulated calcium entry. *Cell Calcium.* **7** (1), 1-12. (1986).
26. Feske, S. CRAC channelopathies. *Pflugers Arch.* **460** (2), 417-435 (2010).
27. Maus, M. *et al.* Missense mutation in immunodeficient patients shows the multifunctional roles of coiled-coil domain 3 (CC3) in STIM1 activation. *Proc Natl Acad Sci U S A.* **112** (19), 6206-6211 (2015).
28. Stathopulos, P.B., Zheng, L., Li, G.Y., Plevin, M.J., & Ikura, M. Structural and mechanistic insights into STIM1-mediated initiation of store-operated calcium entry. *Cell.* **135** (1), 110-122 (2008).
29. Stathopulos, P.B., & Ikura, M. Partial unfolding and oligomerization of stromal interaction molecules as an initiation mechanism of store operated calcium entry. *Biochem Cell Biol.* **88** (2), 175-183 (2010).
30. Dennis, J.W., Lau, K.S., Demetriou, M., & Nabi, I.R. Adaptive regulation at the cell surface by N-glycosylation. *Traffic.* **10** (11), 1569-1578 (2009).
31. Nilsson, T., Au, C.E., & Bergeron, J.J. Sorting out glycosylation enzymes in the Golgi apparatus. *FEBS Lett.* **583** (23), 3764-3769 (2009).
32. Stanley, P. Golgi glycosylation. *Cold Spring Harb Perspect Biol.* **3** (4) (2011).
33. Moremen, K.W., Tiemeyer, M., & Nairn, A.V. Vertebrate protein glycosylation: diversity, synthesis and function. *Nat Rev Mol Cell Biol.* **13** (7), 448-462 (2012).
34. Gerlach, J., Sharma, S., Leister, K., & Joshi, L. In: *Endoplasmic Reticulum Stress in Health and Disease.* Agostinis, P., & Afshin, S., eds., Bristol-Myers Squibb, Syracuse, NY, 23-39 (2012).
35. Pearse, B.R., & Hebert, D.N. Lectin chaperones help direct the maturation of glycoproteins in the endoplasmic reticulum. *Biochim Biophys Acta.* **1803** (6), 684-693 (2010).
36. Stanley, P., & Sundaram, S. Rapid assays for lectin toxicity and binding changes that reflect altered glycosylation in mammalian cells. *Curr Protoc Chem Biol.* **6** (2), 117-133 (2014).
37. Avezov, E., Frenkel, Z., Ehrlich, M., Herscovics, A., & Lederkremer, G.Z. Endoplasmic reticulum (ER) mannosidase I is compartmentalized and required for N-glycan trimming to Man5-6GlcNAc2 in glycoprotein ER-associated degradation. *Mol Biol Cell.* **19** (1), 216-225 (2008).
38. Csutora, P. *et al.* Novel role for STIM1 as a trigger for calcium influx factor production. *J Biol Chem.* **283** (21), 14524-14531 (2008).
39. Kilch, T. *et al.* Mutations of the Ca2+-sensing stromal interaction molecule STIM1 regulate Ca2+ influx by altered oligomerization of STIM1 and by destabilization of the Ca2+ channel Orai1. *J Biol Chem.* **288** (3), 1653-1664 (2013).
40. Williams, R.T. *et al.* Stromal interaction molecule 1 (STIM1), a transmembrane protein with growth suppressor activity, contains an extracellular SAM domain modified by N-linked glycosylation. *Biochim Biophys Acta.* **1596** (1), 131-137. (2002).

41. Mignen, O., Thompson, J.L., & Shuttleworth, T.J. STIM1 regulates Ca2+ entry via arachidonate-regulated Ca2+-selective (ARC) channels without store depletion or translocation to the plasma membrane. *J Physiol.* **579** (Pt 3), 703-715 (2007).
42. Choi, Y.J., Zhao, Y., Bhattacharya, M., & Stathopulos, P.B. Structural perturbations induced by Asn131 and Asn171 glycosylation converge within the EFSAM core and enhance stromal interaction molecule-1 mediated store operated calcium entry. *Biochim Biophys Acta.* **1864** (6), 1054-1063 (2017).
43. Davis, B.G., Lloyd, R.C., & Jones, J.B. Controlled site-selective protein glycosylation for precise glycan structure-catalytic activity relationships. *Bioorg Med Chem.* **8** (7), 1527-1535 (2000).
44. Gamblin, D.P., van Kasteren, S.I., Chalker, J.M., & Davis, B.G. Chemical approaches to mapping the function of post-translational modifications. *FEBS J.* **275** (9), 1949-1959 (2008).
45. Ehrt, S., & Schnappinger, D. Isolation of plasmids from E. coli by alkaline lysis. *Methods Mol Biol.* **235**, 75-78 (2003).
46. Sanger, F., & Coulson, A.R. A rapid method for determining sequences in DNA by primed synthesis with DNA polymerase. *J Mol Biol.* **94** (3), 441-448 (1975).
47. Laemmli, U.K. Cleavage of structural proteins during the assembly of the head of bacteriophage T4. *Nature.* **227** (5259), 680-685 (1970).
48. Bell, D.J. Mass spectrometry. *Methods Mol Biol.* **244**, 447-454 (2004).
49. Domon, B., & Aebersold, R. Mass spectrometry and protein analysis. *Science.* **312** (5771), 212-217 (2006).
50. Farrow, N.A. *et al.* Backbone Dynamics of a Free and a Phosphopeptide-Complexed Src Homology-2 Domain Studied by N-15 Nmr Relaxation. *Biochemistry.* **33** (19), 5984-6003 (1994).
51. Kay, L.E., Keifer, P., & Saarinen, T. Pure Absorption Gradient Enhanced Heteronuclear Single Quantum Correlation Spectroscopy with Improved Sensitivity. *Journal of the American Chemical Society.* **114** (26), 10663-10665 (1992).
52. Delaglio, F. *et al.* NMRPipe: a multidimensional spectral processing system based on UNIX pipes. *J Biomol NMR.* **6** (3), 277-293 (1995).
53. Masse, J.E., & Keller, R. AutoLink: automated sequential resonance assignment of biopolymers from NMR data by relative-hypothesis-prioritization-based simulated logic. *J Magn Reson.* **174** (1), 133-151 (2005).
54. Monticelli, M., Ferro, T., Jaeken, J., Dos Reis Ferreira, V., & Videira, P.A. Immunological aspects of congenital disorders of glycosylation (CDG): a review. *J Inherit Metab Dis.* **39** (6), 765-780 (2016).
55. An, H.J., Kronewitter, S.R., de Leoz, M.L., & Lebrilla, C.B. Glycomics and disease markers. *Curr Opin Chem Biol.* **13** (5-6), 601-607 (2009).
56. Wani, W.Y., Chatham, J.C., Darley-Usmar, V., McMahon, L.L., & Zhang, J. O-GlcNAcylation and neurodegeneration. *Brain Res Bull.* (2016).
57. Haines, A.M., Tobe, S.S., Kobus, H.J., & Linacre, A. Properties of nucleic acid staining dyes used in gel electrophoresis. *Electrophoresis.* **36** (6), 941-944 (2015).

